

Induction Motor Control By Employing SEPIC Converter for electrical applications

N Vengadachalam¹, Shaik Naheda Begam², M Sadhana², B Deepthi²

¹Professor, Department of EEE, Malla Reddy Engineering College for Women, Hyderabad, Telangana, India.

²UG Scholar, Department of EEE, Malla Reddy Engineering College for Women, Hyderabad, Telangana, India.

Abstract:

Conventional Buck, Boost and Buck-Boost converters are not suitable for low and medium voltage induction motor drive applications. Moreover, these DC-DC converters not suitable for power factor correction, constant output voltage and to reduce harmonic distortion. In order to avoid these drawbacks, this project is used to control the speed of three phase induction motor by employing sepic converter. The sepic converter is used to boost the input voltage. The boosted dc voltage is applied to the three phase inverter. This three phase VSI operates at 120 degree mode of operation. Three phase induction motor speed depends on the frequency of inverter.

Introduction:

The solar energy can be converted into useful electrical energy using photo-voltaic effect [1]. In the PV panel, each cell gives 23V and total of 20cells are associated in series to get an average voltage of 443V. This generated voltage is supplied as an input for the three major converters namely SEPIC, Landsman and Zeta converters. The MPPT technique is used to extract the maximum solar power from PV panels. The MPPT technique is applied to generate the adjustable switching cycle for the DC-DC Converters. Thereby, it controls the output voltage obtained by the PV Panel. The three DC-DC converters work as a buck, boost and buck-boost converters depends on the duty ratio and the application requirement. The converters output waveform accuracy mainly depends on the selection of capacitor, Inductor and switches. The major

advantages of SEPIC converter are low input current pulsating and less electromagnetic interference [2-3]. The Zeta converters are used for solar energy generation systems for soft starting of the industrial drive and noninverting continuous load voltage applications [4]. The gate signal is given to drive each DC-DC converter and its duty cycle generated from the solar MPPT control. Here, P&O control technique is used to increase the energy utilization of solar PV [5-6]. The P&O is a simple MPPT technique and it does not need the past data of solar panel characteristics for measuring the intensity of solar cell junction temperature. The P&O algorithm measures the solar panel output parameters before and after perturbation. From the perturbation, if the solar PV power increases the P&O technique, it continues to perturb the PV panel in a similar way or else it perturbs the system in reverse direction [7]. The DC-DC converter output voltage is given to three

phase Sine Pulse Width Modulation (SPWM) based VSI. These three-phase inverter pulses are generated on the basis of stator voltage, frequency and reference speed of IM. The high frequency Metal oxide semiconductor field effect transistor (MOSFET) switches are used for the inverter to convert DCAC voltage to run the motor at required speed. The IM are used in fans, centrifugal pumps and low inertia loads which are frequently starting and stopping [8]. To drive the IM at required speed, the three-phase inverter RMS output voltage taken as 440V. In this article, section-II is describing 443V solar panel design and section-III gives design and control of different types of DC-DC converters. The SPWM is used to generate the switching pulses for three phase VSI and its behavior explained in section IV. The design of IM drive is explained in section V and finally, section VI & VII gives the simulated results and conclusion. The entire system performance is analyzed by using MATLAB/Slink software. The basic diagram of solar array fed IM drive system is described in Fig.1.

The PV array operation is analyzed by the use of single diode equivalent circuit and is described in “Fig.2”. The I-V characteristics of a solar array is explained at different irradiancies (600, 200 and 1000W/m²) by the use of superposition of dark and sunlight current and it is shown in “Fig.3”. Due to illumination of sunlight I-V characteristics shifts from first to the fourth quadrant. “Fig.2” is used together with the following set of equations to explain the I-V characteristics of the solar array [9]. The solar panel parameters are summarized in Table 1.

$$I_L = I_{ph} - I_{d0} - I_{sh} \quad (1)$$

$$I_{ph} = I_{sc} + K_t \times (T_{op} - T_{ref})S \quad (2)$$

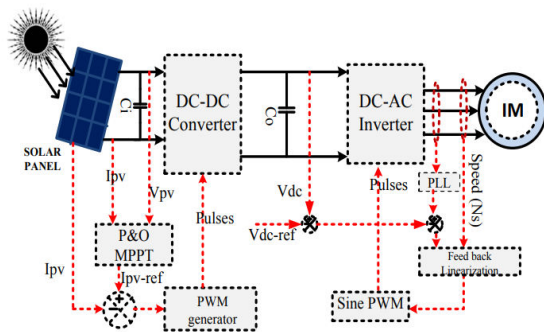


Fig.1. Block diagram of solar PV induction motor drive system

I. SINGLE DIODE EQUIVALENT SOLAR MODEL

$$m = \frac{q * V_{oc}}{N_s * A * K * T_{op}} \quad (3)$$

$$I_0 = I_{rs} * \left(\frac{T_{op}}{T_{ref}}\right)^3 * \exp\left[\left(\frac{q * E_s * N_s}{K * A}\right) * a\right] \quad (4)$$

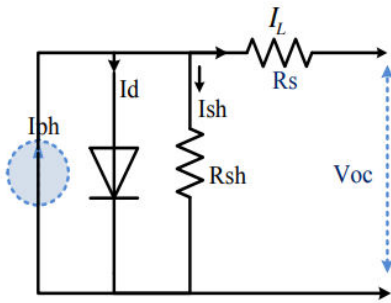


Figure 2. Basic single diode PV-module

$$a = \left(\frac{1}{T_{op}} - \frac{1}{T_{ref}}\right) \quad (5)$$

$$I = N_p I_{ph} - N_p I_0 \times (e^{bc} - 1) \quad (6)$$

Where,

$$b = \frac{q}{N_s * A * K}, \quad c = V + IR_s$$

The single diode equivalent is shown in Fig.2 and it helps to determine the I-V and P-V curves, as a function of operating temperature and solar radiations and it is shown in Fig.3. The Power generated by the PV varies with solar irradiation and intensity of temperature. The variation of solar parameters affects the I-V and P-V characteristics of the solar system. In order to achieve higher efficiency of the solar energy generation, it is essential to maintain a balance between PV generation and load, so that the operating point of PV generation coincides with the Maximum Power Point (MPP) [10].

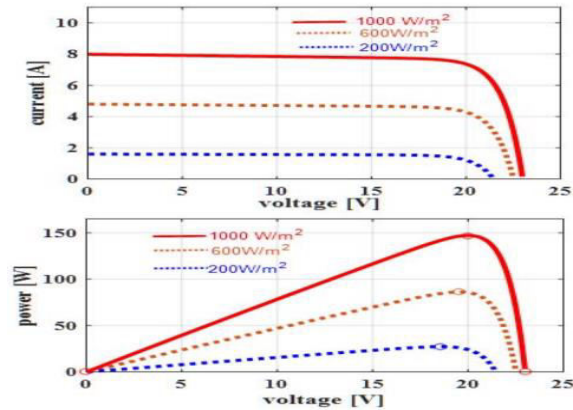


Figure 3. Nonlinear characteristics of PV module

To obtain maximum power, the solar modules are operated at MPPT under different environmental conditions. The four parameters series resistance (R_s), shunt resistance (R_{sh}), short circuit current (I_{sc}) and open circuit voltage (V_{oc}) are required to determine the MPPT point.

Table 1. Solar panel design parameters

S.No	Parameters	Value
1	Maximum peak power (P_{MPPT})	147 (W)
2	No. of parallel strings (N_p)	2
3	Series string (N_{cell})	30
4	Cells per module	60
5	Open circuit voltage (V_{oc})	23.5 (V)
6	Short circuit current (I_{sc})	7.84 (A)
7	Maximum peak voltage (V_{MPPT})	20 (V)
8	Maximum peak current (I_{MPPT})	7.35(A)
9	Temperature co. efficient of V_{oc}	-0.36099 ($^{\circ}C$)
10	Temperature co. efficient of I_{sc}	0.102 ($^{\circ}C$)
11	Standard temperature (T)	25% ($^{\circ}C$)
12	Irradiances (S)	600,200,1000 (W/m^2)
13	Ideality factor	0.6214
14	Shunt resistance (R_{sh})	69.5035 (Ω)
15	Series resistance (R_s)	0.00154 (Ω)

The P&O algorithm works at different environmental conditions for improving the overall system energy utilization and it gives duty cycle to DC-DC converter [11]. The solar panel parameters are same for three DC-DC converters operation.

II. ANALYSIS OF DC-DC CONVERTERS

Based on the intensity of solar radiations, the solar PV voltage will fluctuate. In order to overcome this, buck/boost converter have been employed. These DC-DC converters are mainly used to change the voltage levels, optimizing the losses from the obtained solar voltage level. The three converters and their performance are analyzed for solar PV IM drive application.

A. Operation of SEPIC converter

The duty ratio of SEPIC for ideal and practical condition is calculated as,

$$D_{ideal} = \frac{V_{dc}}{V_{in} + V_{dc}} \quad (9)$$

$$D_{practical} = \frac{V_0 + V_D}{V_{in} + V_0 + V_D} \quad (10)$$

Here V_{dc} and V_{in} are the output and input voltages of SEPIC. V_{MPPT} is the maximum peak volatge of PV panel, which is the input to SEPIC converter, V_D is the diode voltage drop and D is the duty ratio of the converter. The circuit parameters are considered for SEPIC converter which is to operate in continuous operation mode and these parameters are evaluated by using equations (9), (10) and (11). The circuit of SEPIC converter fed PV IM drive is described in “ Fig.4” .

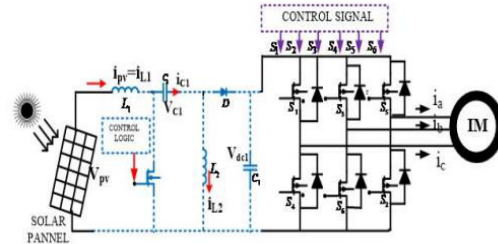


Figure 4. Block diagram of SEPIC converter fed PV SIMD system

$$L_2 = \frac{(1-D) \times V_{dc}}{f \times \Delta I_{L_1}} \quad (9)$$

$$L_1 = \frac{D \times V_{PV}}{f \times \Delta I_{L_1}} \quad (10)$$

$$C_1 = \frac{D \times I_{OUCT}}{f \times \Delta V_{C_1}} \quad (11)$$

Based on the above inductor and capacitor parameters, the SEPIC converter work in Continuous Conduction Mode (CCM) of operation. If the switch is “ ON” inductors L_1 , L_2 starts charging by V_{dc} and V_{C1} and when the switch is “ OFF” capacitors C_1 , C_2 starts discharging by L_2 [12-13].

B. Operation of Landsman converter

The main objective of Landsman converter is to optimize the solar panel output voltage and to give secure and smooth starting of the IM. Compare to Zeta, this converter gives better performance for IM drive application [14]. The parameters of Landsman are selected to operate in the CCM of operation and those parameters are evaluated by using exultations (12), (13) and (14). If the switch is “ON” in Landsman converter, the diode gets reverse biased and its supply input current flows through the switch. If V_{c1} is more than V_{dc} , capacitor C_1 discharges through the switch and input energy gets the

transfer to the output. The Landsman converter fed solar IM drive system is shown in “Fig.5”.

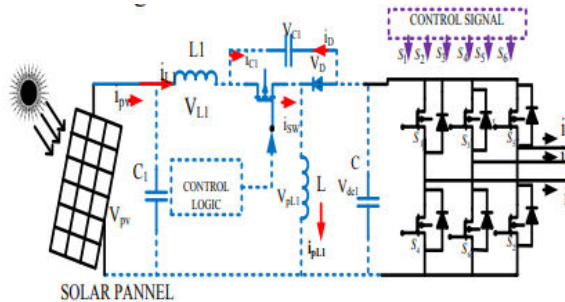


Figure 5. Block diagram of Landsman converter fed PV IMD sys

Whenever the switch is “ OFF” , the diode gets forward biased and inductor current i_{L1} flows through the diode. Landsman converters inductor peak to peak current ripple, input capacitor current and corresponding peak to peak voltage ripples under CCM of operation are calculated by the following equations [14-15],

$$\Delta i_{L1} = \frac{\Delta V_{C1} * T}{8L_1} \quad (12)$$

$$i_{C1} = \frac{\Delta V_{C1} * C_1}{(1-D)*T} \quad (13)$$

$$\Delta V_{C1} = \frac{(1-D)T * I_{L1}}{C_1} \quad (14)$$

From the above equation (12), (13) and (14) the peak to peak current ripple is derived as,

$$\Delta I_{L1} = \frac{(1-D)T^2 * I_{L1}}{8C_1} \quad (15)$$

The duty cycle ratio, capacitor C1, inductors L1 and L2 are derived as,

$$D = \frac{V_{dc}}{V_{dc} + V_{in}} \quad (16)$$

$$C_1 = \frac{D * i_{dc}}{f * \Delta V_{C1}} \quad (17)$$

$$L_1 = \frac{D * i_{dc}}{8f^2 * \Delta I_{L1} * C_1} \quad (18)$$

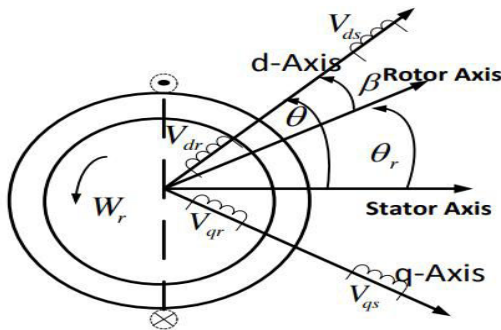
$$L_2 = \frac{D * V_{dc}}{f * \Delta I_{L2}} \quad (19)$$

Based on the above inductor and capacitor values the SEPIC converter works in CCM of operation. If the switch is “ ON” inductors L1, L2 starts charging by V_{dc} and V_{C1} and when the switch is “ OFF” capacitors C1, C2 starts discharging through L2 [12-13]. The SEPIC and Landsman converters are applied for correcting the power factors of the supplies in both continuous and discontinuous mode of operation. However, all these converters have certain limitations. They cannot protect against overload and short-circuit current. A major practical difficulty associated with these converters is handling of magnetic inrush current. All these above-mentioned drawbacks can easily overcome by using Zeta converter [16].

III. DESIGN OF IM DRIVE

The three-phase IM is highly effective for a broad scope of applications because of its strong construction and less price. The behavior of IM is described by their voltage, current, speed and torque parameters. The asynchronous machines are wound rotor, double squirrel cage and squirrel motors. There are designed by using stationary reference frame

theory because of its easy design and mathematical calculations [20]. The coefficient of differential equations gives the time-varying behavior of IM. A mathematical modeling of such a time-varying induction machine system design tends to be difficult because of the flux linkages, induced currents and voltages vary continuously as the IM is in relative speed. The Clark's and Park's transformations are used to convert time-varying quantity to stationary quantity. In rotating reference frame theory, two controllers are required to control the IM and in stationary reference frame theory, only one controller is used [21-22]. Hence, most of the induction machines are designed by using stationary reference frame theory and is shown in " Fig.7" .



The park's transformation matrix is followed as,

$$I_{0dq} = A_{\theta} * I_{abc}$$

$$A_{\theta} = \frac{2}{3} \times \begin{bmatrix} \frac{+1}{2} & \frac{+1}{2} & \frac{+1}{2} \\ \cos \theta_r & \cos(\theta_r - \lambda) & \cos(\theta_r + \lambda) \\ \sin \theta_r & \sin(\theta_r - \lambda) & \sin(\theta_r + \lambda) \end{bmatrix}$$

Where, T_r is the rotation angle and O is the displacement angle. In stationary reference frame

theory, the zero sequence components are involved to balance the unbalance three-phase quantities. From the dq frame theory, the IM stator and rotor voltages are derived as follows,

$$V_{dst} = r_{st} * i_{dst} + A \psi_{dst}$$

$$V_{qst} = r_{st} * i_{qst} + A \psi_{qst}$$

$$V_{drt} = r_{rt} * i_{drt} + A \psi_{drt} - \psi_{qrt} \omega_r$$

$$V_{qrt} = r_{rt} * i_{qrt} + A \psi_{qrt} + \psi_{drt} \omega_r$$

Where, V_{dst} , V_{drt} , V_{qst} and V_{qrt} are the direct and quadrature axis voltage components and r_{st} and r_{rt} are the stator and rotor resistances and A is the differential coefficient. From equation, the matrix notation of dq reference frame theory is as follows,

$$\begin{bmatrix} \psi_{dst} \\ \psi_{drt} \\ \psi_{qst} \\ \psi_{qrt} \end{bmatrix} = \begin{bmatrix} L_{ss} & L_m & 0 & 0 \\ L_m & L_{rr} & 0 & 0 \\ 0 & 0 & L_{ss} & L_m \\ 0 & 0 & L_m & L_{rr} \end{bmatrix} \begin{bmatrix} i_{dst} \\ i_{drt} \\ i_{qst} \\ i_{qrt} \end{bmatrix}$$

In stationary reference frame theory, the d, q axes don't rotate. So, the rotation angle T is zero and corresponding AT is also zero. From the vector notation,

$$\beta = \theta - \theta_r = -\theta_r, A_{\beta} = -A\theta_r = -\omega_r$$

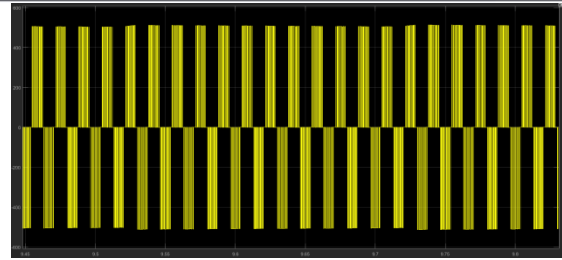
From equation above, the stationary direct and quadrature axis voltages are derived as,

$$V_{dst} = r_{st} * i_{dst} + A \psi_{dst}$$

$$V_{qst} = r_{st} * i_{qst} + A \psi_{qst}$$

$$V_{drt} = r_{rt} * i_{drt} + A \psi_{drt} - \psi_{qrt} \omega_r$$

$$V_{qrt} = r_{rt} * i_{qrt} + A \psi_{qrt} + \psi_{drt} \omega_r$$



Inverter output voltage

IV. Simulation results

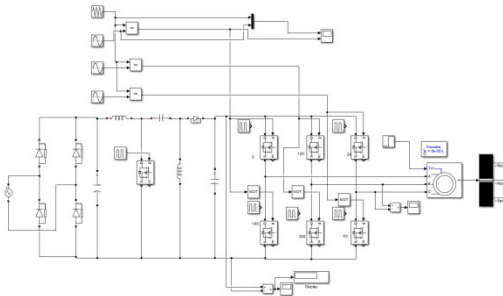
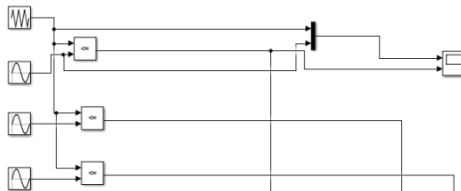
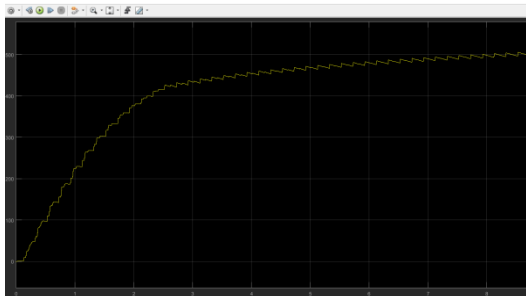


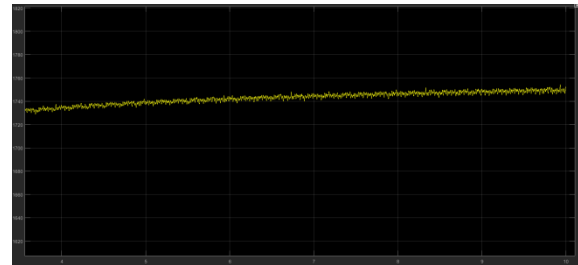
Fig main circuit simulation diagram



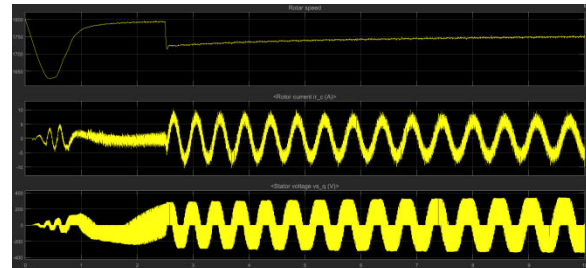
Inverter controlling



SEPIC converter output voltage



Motor speed



Motor speed, Rotor current and Stator voltage

V. Conclusion

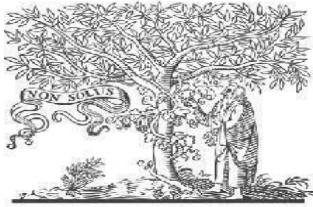
Comparative analysis is presented in this project on application of SEPIC, Boost converters for solar PV fed IM drives and its analysis simulation results are given it is observed that, SEPIC converter gives high constant output voltage gain, less current and reduced total harmonic distortion for PV fed IM compare to

Boost converter. Moreover, SEPIC converter fed induction motor speed is high compare to other DC-DC converters. From this simulation analysis SEPIC converter fed PV induction drive system working with less loss and high converter efficiency.

VI. References

- [1] A. Mohammed., Bashar Zahawi, and J. David . Atkinson. "Assessment of perturb and observe MPPT algorithm implementation techniques for PV pumping applications." *IEEE transactions on sustainable energy* 3.1 (2012): 21-33.
- [2] Onur. Kircioğlu,Unlu. Murat and Sabri Çamur. "Modeling and analysis of DC-DC SEPIC converter with coupled inductors." *Industrial Electronics International Symposium on. IEEE*, 2016.
- [3] S. Mishra, A. Kumar, and Bhim Singh, "Solar PV powered SRM driven water pumping system using Landsman converter." *Power Electronics, Drives and Energy Systems (PEDES), 2016 IEEE International Conference on. IEEE*, 2016.
- [4] Andrade,H. L. Hey, and S. Martins. "Non-pulsating input and output current C^k, SEPIC, Zeta and Forward converters for high-voltage stepup applications." *Electronics Letters* 53.18 (2017): 1276-1277.
- [5] Alik. Rozana, A. Jusoh, and Tole Sutikno. "A Study of Shading Effect on Photovoltaic Modules with Proposed P&O Checking Algorithm." *International Journal of Electrical and Computer Engineering* 7.1 (2017): 29.
- [6] Yeung. Ryan Shun-cheung, et al. "A global MPPT algorithm for existing PV system mitigating suboptimal operating conditions." *Solar Energy* 141 (2017): 145-158.
- [7] D. Hanen, et al. "Critical factors affecting the photovoltaic characteristic and comparative study between two maximum power point tracking algorithms." *International Journal of Hydrogen Energy* 42.13 (2017): 8689-8702.
- [8] D. Emad, Antero and Arkkio. "A general model for investigating the effects of the frequency converter on the magnetic iron losses of a squirrel-cage induction motor." *IEEE Transactions on Magnetics* 45.9 (2009): 3303-3315.
- [9] Ikegami. "Estimation of equivalent circuit parameters of PV module and its application to optimal operation of PV system." *Solar energy materials and solar cells* 67.1 (2001): 389-395.
- [10] N. Mohamed., Peter Sergeant, and M. Essam. Rashad. "Design of low cost and efficient photovoltaic pumping system utilizing synchronous reluctance motor." *Electric Machines and Drives Conference (IEMDC), 2017 IEEE International. IEEE*, 2017.

COPY RIGHT



ELSEVIER
SSRN

2021IJIEMR. Personal use of this material is permitted. Permission from IJIEMR must be obtained for all other uses, in any current or future media, including reprinting/republishing this material for advertising or promotional purposes, creating new collective works, for resale or redistribution to servers or lists, or reuse of any copyrighted component of this work in other works. No Reprint should be done to this paper, all copy right is authenticated to Paper Authors

IJIEMR Transactions, online available on 20th Apr 2022.

Link : <https://ijiemr.org/downloads/Volume-11/Issue-04>

DOI: 10.48047/IJIEMR/V11/I04/19

Title: Induction Motor Control By Employing SEPIC Converter for electrical applications

volume 11, Issue 04, Pages: 106-115

Paper Authors: **N Vengadachalam, Shaik Naheda Begam, M Sadhana, B Deepthi**



